Talanta 79 (2009) 978–983

Contents lists available at ScienceDirect

Talanta

journal homepage: www.elsevier.com/locate/talanta

Evidences of turbulent mixing in multi-pumping flow systems

Paula R. Fortes [a], Mario A. Feres [a], Milton K. Sasaki [a], Evandro R. Alves [a], Elias A.G. Zagatto [a,*], João A.V. Prior [b], João L.M. Santos [b], José L.F.C. Lima [b]

[a] Centro de Energia Nuclear na Agricultura, Universidade de São Paulo, P.O. Box 96, Piracicaba 13400-970, Brazil
[b] REQUIMTE, Departamento de Química-Física, Faculdade de Farmácia, Universidade do Porto, Rua Anibal Cunha 164, Porto 4050-047, Portugal

ARTICLE INFO

Article history:
Available online 13 February 2009

Keywords:
Flow analysis
Multi-pumping
Turbulent mixing
Sample dispersion
Pulsed flow

ABSTRACT

Multi-pumping flow systems exploit pulsed flows delivered by solenoid pumps. Their improved performance rely on the enhanced radial mass transport inherent to the pulsed flow, which is a consequence of the establishment of vortices thus a tendency towards turbulent mixing.

This paper presents several evidences of turbulent mixing in relation to pulsed flows, such as recorded peak shape, establishment of fluidized beds, exploitation of flow reversal, implementation of relatively slow chemical reactions and/or heating of the reaction medium. In addition, Reynolds number associated with the GO period of a pulsed flow is estimated and photographic images of dispersing samples flowing under laminar regime and pulsed flow conditions are presented.

1. Introduction

Laminar flow is an intrinsic characteristic of flow analysis [1,2]. Inside a narrow bore open tubular reactor, the linear velocity of a fluid element of the sample zone located at the axis of the tube is about twice the average linear flow velocity, whereas the linear velocities of fluid elements adjacent to the tube walls approach zero [3]. In this way, concentric iso-concentration cylinders traveling at different linear velocities are established. This convective effect may lead to a pronounced sample axial dispersion, thus increased sample broadening. It is the main source of carryover [4,5] and should be minimized for improving sensitivity, wash time and/or sampling rate. Consequently, different strategies for minimizing sample broadening have been proposed, leading often to alterations in the involved laminar flow regime.

In segmented flow analysis, sample broadening is lessened and mixing conditions are improved because the addition of successive air bubbles results in a circulating flow pattern inside the liquid segments, and vortices are established [6]. The radial mass transport is then improved.

In unsegmented flow analysis relying on laminar flows, sample broadening is more pronounced, as axial dispersion is more likely to occur. The effect is beneficial for some applications requiring large sample dispersion [7] and/or exploiting concentration gradients [8,9]. For most applications however, it is detrimental and should be minimized.

In this regard, the reactor should be as short as possible yet enough for providing good mixing conditions. Use of coiled tubular reactors reduces sample broadening, as the involved fluid elements cannot be displaced following the parallel trajectories inherent to the typical laminar flow regime, thus establishing secondary flows [3,10]. Use of knitted (or 3D) reactors results in an analogous yet more pronounced effect [11], and packed bed reactors [12] (also immobilized reagents, resin mini-columns, monolithic columns and enzyme cartridges) or single bead string reactors [13] are also advantageous, as the intrinsic channeling effects play a beneficial role on system performance.

Letting the flowing stream to rapidly pass through very thin orifices can attain turbulent-like flows [14,15]. The strategy has been seldom used, probably because of the high pressure-drop involved thus the need for an HPLC pump. Inclusion of stirred chambers [16] and special confluence connectors [17] into the manifold also improves mixing conditions. Floating solid particles formed as reaction products or added as solid suspensions [18] or beads [19], are also beneficial to reduce sample broadening [20]. Use of supercritical fluids as means to improve radial mixing by exploiting fugacity was also investigated [21], but the flow system required special components and carbon dioxide seems to be the only chemical species suitable for this purpose. Gaseous carrier streams were already exploited in relation to gas–solid [22] or gas–liquid interfaces [23] but, in spite of the improvement in mixing conditions, the number of applications to date is relatively low [24].

Beneficial aspects of pulsed flows [25] have been noted mainly in relation to the multi-pumping flow systems, MPFS [26]. Successive solution volumes are suddenly inserted as pulses into the manifold (usually by means of solenoid or step-wise piston pumps), establishing a pulsed flow. Turbulent mixing is approached dur-

* Corresponding author.
E-mail address: ezagatto@cena.usp.br (E.A.G. Zagatto).

0039-9140/$ – see front matter © 2009 Elsevier B.V. All rights reserved.
doi:10.1016/j.talanta.2009.01.062

ing the very short GO periods whereas the main stream is stopped between each pulse (STOP period) [25]. Vortices are formed during the GO period, enhancing the radial mass transport, hence allowing the design of improved analytical procedures [27]. In general, the manifolds are very simple, allowing enhanced figures of merit to be attained. A comparison between flow systems relying on pulsed or laminar flows was recently reported [28], but a deeper investigation of pulsed flows with emphasis to situations where they behave as turbulent-like flows is still needed.

The main purpose of the present work was than to highlight evidences of turbulent mixing in MPFS. To this end, aspects related to recorded peak shapes, slow chemical reactions, improved heating, fluidized beds and flow reversals are discussed. In addition, the Reynolds number is roughly estimated and images of the flowing samples are presented.

2. Recorded peak shapes

Shape of the recorded peak highlights the sample broadening, which is less pronounced in MPFS relatively to other unsegmented flow systems, due to the more efficient radial mass transport involved [28]. Thus, low axial dispersion, improved sampling rate and skew peaks have been emphasized in relation to MPFS [29,27], and these aspects can be regarded as an evidence of turbulent mixing.

In order to corroborate this evidence, a multi-commuted (MCFS) and a multi-pumping (MPFS) flow systems relying on laminar or pulsed flows, respectively, were designed as similar as possible (Fig. 1), the only difference between them being the propeller unit, either a model IPC-8 Ismatec peristaltic pump or two 25-μL Bio-Chem Valve Inc. solenoid pumps. For both systems, flow rate, reactor length and sample volume were set as 2.0 mL min^{-1}, 300 cm and 200 μL, respectively. A model USB2000 UV-vis Ocean Optics spectrophotometer with optical fibers was used with an acrylic Z-shaped flow cell [30] (inner volume: 10 μL, optical path: 10 mm). The time interval for measurements and the wavelength were set as 25 ms and 612 nm. Two MTV-3-N1/4UKG three-way solenoid valves (Takasago Electric Inc., Nagoya, Japan) and Perspex connectors were also used. The reactor and the transmission lines were build-up with 0.8-mm i.d. polyethylene tubing of the non-collapsible wall type. System operation, as well as data acquisition and treatment, were computer controlled (interface card: Advantech PCL-711S; language: Quick Basic 4.5).

For sample introduction into the flow systems, the carrier stream was stopped and the sample solution was directed towards the analytical path at the same flow rate; after the sample selected volume was inserted, the sample stream was stopped and the carrier stream was directed towards the analytical path. To this end, either the three-way valves were switched to direct the solutions towards the analytical path or towards waste (MCFS) or the solenoid pumps were switched on or off (MPFS). The sample volume was defined in terms of sampling time and flow rate (MCFS) or stroke volume and frequency (MPFS).

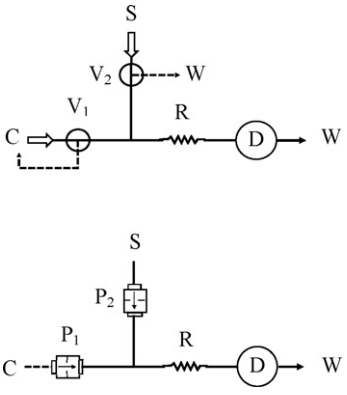

Fig. 1. Flow diagram of the multi-commuted (upper) and multi-pumping (lower) flow systems used for comparing recorded peak shapes. S = sample; C = carrier stream; V_i = three-way solenoid valves; P_i = solenoid pumps; white arrows = sites where peristaltic pump is applied; R = tubular reactor; D = detector; W = waste. Solid and traced lines = present and alternative flow paths. For details, see text.

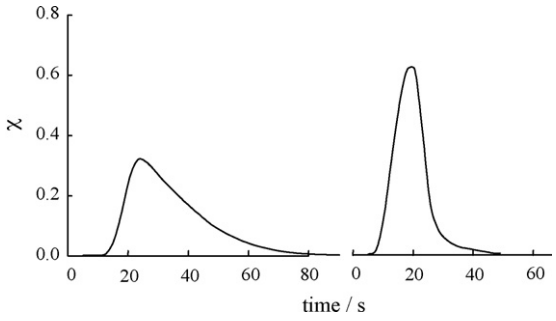

Fig. 2. Recorder tracings obtained with the multi-commuted (left) and multi-pumping (right) flow systems. Figure refers to 25 mg L^{-1} BCG. χ = volumetric fraction [46]. For details, see text.

Bromocresol green solutions (10.0–50.0 mg L^{-1} BCG, also 0.01 mol L^{-1} $Na_2B_4O_7$) were used to mimic the sample. A 0.01 mol L^{-1} $Na_2B_4O_7$ solution was used as the sample carrier stream in order to minimize the establishment of undesirable pH gradients, which might lead to a pronounced Schlieren effect.

The beneficial influence of pulsed flow can be gathered from Fig. 2. Height and width of the recorded peak, as well as washing time, were significantly improved, meaning better sensitivity and sampling rate. Moreover, the mean sample residence time in the analytical path [31] was shorter for MPFS. In fact, as laminar flow is not involved, the delay usually undergone by the flowing sample under laminar flow conditions became less pronounced. One can then conclude that peak shape is an evidence of the improved radial mass transport inside a pulsed flow.

3. Slow chemical reactions

In flow-based analytical procedures relying on relatively slow chemical reactions, the degree of reaction completion, thus sensitivity is closely related to the mixing conditions and to the radial mass transport involved. If these aspects are more favorable, the effective mean available time for reaction development is higher because mixing between analyte and reagent is faster, thus sample/reagent interactions starts earlier. This is the main reason why sensitivity of the spectrophotometric determination of phosphate in soil extracts [28] and the chemiluminometric determination of ammonium in natural waters [32] underwent pronounced improvements when pulsed rather than laminar flows were exploited. Besides the involved better mixing conditions, higher inner pressure and lower sample dispersion played also a pronounced role in sensitivity enhancement.

The beneficial features arising from implementation of relatively slow physico-chemical processes in MPFS [28,33] constitute themselves in another evidence of turbulent mixing in these flow systems.

4. Improved heating

Efficiency of heat transference from a water bath towards a reactor immersed into it is also an indicative of turbulent mixing. In MPFS, this transference is more efficient in relation to other unsegmented flow systems: the chaotic movement of the fluid elements

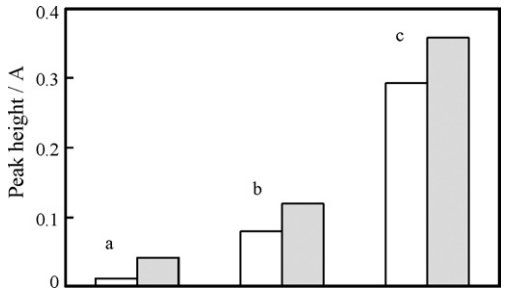

Fig. 3. Height of the peaks recorded for a 0.25% (w/v) glucose solution handled in the MCFS (empty bars) and MPFS (filled bars). Data taken from Ref. [35]; *a*, *b*, *c* = 80, 90 and 98 °C (temperature of the water bath inside which the main reactor was immersed).

and the enhanced radial mass transport during the GO period, lead to a fast and efficient homogenization of the flowing sample. On the other hand, heat transference under laminar flow conditions is worse, as the iso-concentration concentric cylinders close to the inner tube walls are the fluid elements more efficiently heated [34]: transference of heat towards the central streamlines is impaired due to slow radial mass transport involved. In addition, the sample portions near the tube axis are displaced at a linear velocity higher than the averaged flow velocity, thus becoming less heated and acting as a refrigerating agent.

The better heat transference inside a pulsed flow was noted in relation to the spectrophotometric determination of total reducing sugars involving the temperature-dependent processes of sucrose hydrolysis and sugar alkaline degradation [35]. Development of the involved processes was proportional to the height of the recorded peak, being always more complete under conditions of pulsed flows relatively to laminar flow conditions (Fig. 3). This aspect demonstrates again the occurrence of turbulent mixing inside a pulsed flow.

5. Flow reversal

In flow systems with flow reversal [36], the sample zone is initially pushed forwards during a pre-selected time interval and then backwards. With this strategy, it is possible for the sample to pass through the detector before and after flow reversal in order to be monitored twice, as originally demonstrated in the kinetic determination of glucose in clinical samples [37]. Also, flow reversal is a key *modus operandi* of the sequential injection analyzer [38]. Moreover, the sample zone can undergo a forward/backward motion when multiple flow reversals are performed, allowing the control of dispersion and variation of effective reactor length [39,40], thus improving the sample/reagent interactions. Efficient mixing is then attained.

Influence of flow reversal in sample dispersion is affected by turbulent mixing. Under laminar flow conditions (*i.e.* no turbulent mixing), sample broadening results mainly from the establishment of the above-mentioned iso-concentration concentric cylinders flowing at different linear velocities. Dispersion is continuously increased during forward motion of the sample zone, as the cylinders are continuously stretched. After flow reversal, the cylinders tend to shrink, restoring the original sample distribution. Inside a pulsed flow, however, de-convolution of the sample zone might not be achievable after flow reversal. Under conditions of efficient radial mass transport and better mixing conditions, the sample zone becomes more homogeneous and flow reversal does not play a significant role.

In order to demonstrate these antagonistic effects, thus providing an additional evidence of turbulent mixing in pulsed flow, a multi-pumping and a multi-commuted flow systems with optional

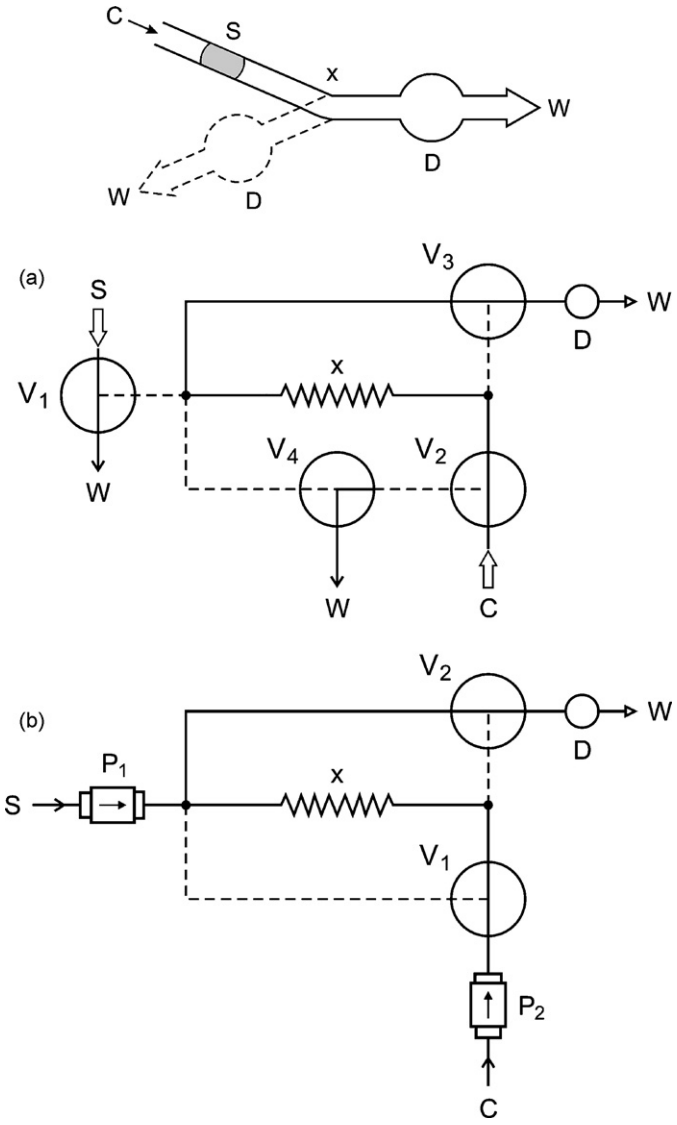

Fig. 4. Didactic presentation (upper) and flow diagrams (lower) of the multi-commuted (a) and multi-pumping (b) systems for investigating influence of flow reversal. Symbols as in Fig. 1; x = reactor median point.

flow reversal were designed as similar as possible (Fig. 4), and their components are described in Section 2. The only difference between them was the flow pattern, as the 4a and 4b systems used peristaltic or solenoid pumps as fluid propeller devices. When flow reversal was not aimed, the sample zone flew through the entire reactor towards detection. Alternatively, the sample zone was pushed to reach only the reactor half; the flow was then reversed, and the sample flew again through the already traveled reactor portion towards detection. In this way, the total traveled distance was maintained regardless if flow reversal was exploited or not.

The 4a system was operated as follows. In the situation specified in the figure, the carrier stream and the sample solutions flew towards detection and waste, respectively. If required, sample replacement was done in this situation. Switching V_1–V_4 valves to the alternative position during a preset time interval intercalated the selected sample volume into the analytical path and directed the carrier stream towards recycling. After sample insertion, V_1 and V_4 valves were switched back to situation in Fig. 4a, allowing the inlet of the sample carrier stream into the analytical path. The originated sample zone was pushed towards detection in a direct manner. Alternatively, all valves could be switched to origi-

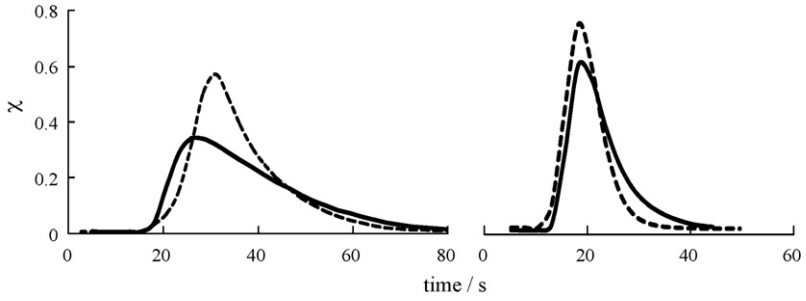

Fig. 5. Influence of flow reversal on recorded peak shape for MCFS (left) and MPFS (right). Figure refers to 25 mg L^{-1} BCG solution inserted into the flow system in Fig. 4 (total flow rate = 2.0 mL min^{-1}, reactor length = 200 cm; sample inserted volume = 100 μL); χ = volumetric fraction; traced and solid lines = situations with and without flow reversal.

nal position when the sample reached reactor half point (x—Fig. 4), promoting flow reversal thus directing the sample zone towards detection in an indirect manner. The 4b system was analogously operated. P_1 and P_2 pumps were accountable for propelling the sample and carrier solutions and V_1 and V_2 valves, for stream directing and detector leaping [41].

Reproducible results were obtained with the flow systems in Fig. 4. Relative standard deviations <1% and <3% for peak height and area were estimated after three repetitive sample handling; these uncertainties were not affected by flow reversal. This is a remarkable result, as it assesses the performance of flow system involving flow reversal such as *e.g.* the sequential injection analyzer.

Flow reversal proved to be a suitable strategy to confirm that turbulent mixing is inherent to MPFS. In fact, differences in sample broadening and washing time caused by flow reversal were always more pronounced in relation to MCFS (Fig. 5) due to the possibility of peak de-convolution caused by shrinking of the iso-concentration cylinders typical from the laminar flow regime. On the other hand, influence of flow reversal was less pronounced in relation to MPFS, as the more efficient radial mass transport impaired the peak de-convolution. Consequently, significant differences related to the peak width and washing time (thus sampling rate) were noted. In addition, when flow was reversed the peak shapes tended to approach a Gaussian format, the phenomenon being more pronounced in relation to pulsed flows. More symmetrical peaks were recorded in relation to MPFS, revealing again the turbulent mixing.

Thus, flow reversal can then be better exploited under laminar flow regime. This is an important issue, especially in regard to sequential injection systems. In fact, the sample/reagent interaction is improved during the formation of the stacked sample/reagent zone inside the holding coil, due to the convective effects involved. After flow reversal, sample/reagent interaction continues to be improved, and the total dispersion is minimized in view of the peak de-convolution involved. Although noteworthy, this aspect seems not to be yet investigated in detail.

Influence of sample volume was investigated between 100 and 400 μL; the total distance travelled by the sample was maintained by modifying the inserted volume of the added carrier stream solution after each modification in sample volume. The differences in recorded peak heights due to flow reversal were linearly proportional to the inserted sample volume (Fig. 6), confirming that extent of sample de-convolution is not influenced by the sample volume in a significant manner. One can then infer that, regardless of flow reversal or not, sample dispersion in both parts of the analytical path follows the known injected volume vs. peak height relationship [31].

Influence of flow rate was investigated between 2.0 and 5.0 mL min^{-1}. To this end, either the rotation speed of the peristaltic pump or the pulse frequency of the solenoid pumps was varied. Flow rate played a minor influence on the recorded peak shapes. For MCFS, slight variations in peak heights (<20%) were noted when flow rate was varied regardless if flow reversal was implemented or not. These variations were less pronounced for MPFS, emphasizing the negligible influence of mean flow rate on sample dispersion. This can be explained by recalling that flow rate variations were attained by varying the STOP period, during which no sample dispersion occurs [28].

All the above-mentioned aspects were maintained, yet in a lesser extend when the straight tubular reactor was coiled. The effect became more evident in relation to the laminar flow, as reactor coiling improves the radial mass transport. On the other hand, influence of the reactor coiling was less pronounced for MPFS, where the radial mass transport is already efficient.

On can then infer that flow reversal is an important indicative of turbulent mixing inside a pulsed flow.

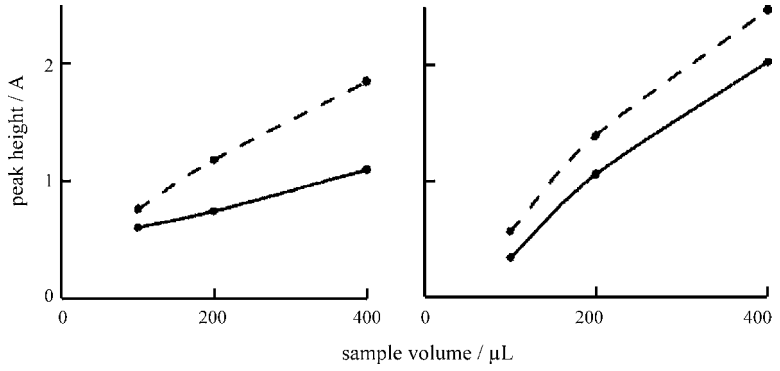

Fig. 6. Influence of sample inserted volume. Figure refers 25 mg L^{-1} BCG solution inserted into to the MCFS (left) and MPFS (right) flow system in Fig. 4 (total flow rate = 2.0 mL min^{-1}, reactor length = 200 cm). Traced and solid lines = situations with and without flow reversal.

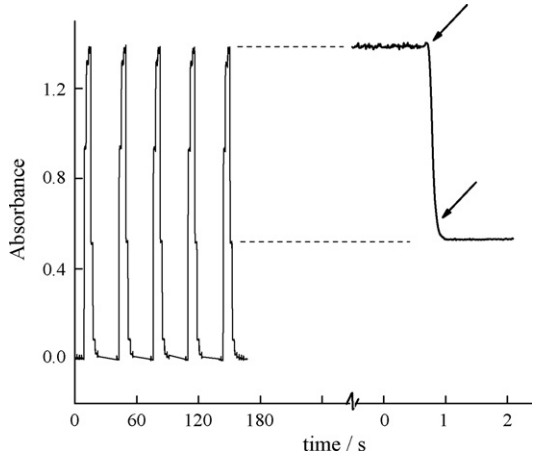

Fig. 7. Part of a peak recorded with the MPFS in Fig. 1 with: sample = 25 mg L^{-1} BCG; stroke value = 25 μL; sample inserted volume = 25 μL; reactor length = 30 cm. Left and right portions refer to low and high speed recording. For details, see text.

6. Reynolds number

Transition from laminar to turbulent flow in a tube is associated with the Reynolds number, Re [42] that can be expressed as [43]:

$$Re = \frac{2\rho Q}{\pi r \mu} \quad (1)$$

where: ρ = mass density of the fluid; Q = flow rate; r = tube radius, μ = dynamic viscosity of the fluid, usually expressed in g cm^{-3}, cm^3 s^{-1}, cm and poise (g cm^{-1} s^{-1}), respectively.

For Re < 2000, flow is laminar; gradual transition between laminar and turbulent flow occurs over the 2000–4000 range, the so-called transition region; turbulence is fully established for Re > 4000.

By taking into account the flow rates and tubing dimensions of a typical unsegmented flow analyzer, one can conclude that laminar is the prevailing flow regime. This is the reason why the expression *"it is unlikely that FIA has ever been carried out with turbulent flow"* appeared in the literature [1]. In fact, for 1-mm i.d. tubing, a 93 mL min^{-1} flow rate might be needed for getting turbulent flow, and this rate is not achievable in ordinary flow systems. Indeed, the flow rate associated with the GO period of a pulsed flow may even surpass this value. Experiments aiming to determine this flow rate, thus allowing a estimation of Re, were then carried out in order to provide an additional assessment of turbulent mixing in MPFS.

To this end, a dye solution (buffered BCG) was inserted into the single-line MPFS in Fig. 1 (lower). In order to minimize damping effects due to tubing plasticity, the reactor was set as short as possible (30 cm) yet enough to permit reproducible measurements to be obtained. The sample was inserted into the carrier stream and transported towards detection. Its passage through the flow cell resulted in a stair-like recorded peak [26] where the horizontal lines corresponded to the STOP periods whereas those approaching verticality corresponded to the GO periods (Fig. 7). As abrupt modifications in the monitored absorbance during the very short GO periods were involved, a low-inner volume flow cell and a fast procedure for data acquisition were needed. Therefore, a model 178.713-QS Hellma flow cell (inner volume: 8 μL) was used, and the time interval for measurements was set as 15 ms. In these experiments, a spectrophotometer USB 1000 converter was used.

The averaged flow rate related to the GO period (Q_{GO}) was estimated as:

$$Q_{GO} = V_P(\Delta t_{GO})^{-1} \quad (2)$$

where V_P = pulse volume (stroke) delivered by the solenoid pump; Δt_{GO} = time interval related to the GO period.

V_P was volumetrically determined [28] and Δt_{GO} was graphically evaluated as the time interval between two successive horizontal lines (Fig. 7). Analysis of this figure permits one to infer that a single step was not enough for proper estimation of Δt_{GO}, as uncertainties in the measurement interval manifested themselves as limiting factors. By considering the same time interval related to five successive recorded peaks, Δt_{GO} was estimated as 0.221 ± 0.028 s. This time domain encompasses 14 absorbance measurements. For a 125-μL stroke volume, flow rate associated to the GO period was determined (Eq. (2)) as:

$$Q_{GO} = (125\ \mu L) \times (0.221 \pm 0.028\ s)^{-1} = 33.9 \pm 4.3\ mL\ min^{-1}$$

For 1.0 mm i.d. tubing a 93 mL min^{-1} flow rate should be required for establishing a turbulent flow regime [1]. This corresponds to 74.4 mL min^{-1} if a 0.8 mm i.d. tubing is concerned. Under this situation Re can be estimated (Eq. (1)) as:

$$Re = \left[\frac{(33.9 \pm 4.3)}{74.4}\right] \times 2000 = 911 \pm 115$$

The actual value of Re is probably higher than 911 ± 115, as effects of the flow cell inner volume, detector response time and sample broadening were not taken into consideration for evaluating Δt_{GO}. Consequently, a higher Δt_{GO} value, thus a lower Re number was determined. Furthermore Δt_{GO} is an averaged value and at the first instants assumes a value much higher than 911 ± 115.

Another aspect to be considered is that during the GO period, the involved high internal pressure leads probably to a temporary modification in tubing geometry, and the effect is compensated (relaxation) during the initial portion of the STOP period. The phenomenon is evident in Fig. 7. The tendency towards accommodation manifests itself immediately after the GO period as slight decrease in the monitored absorbance, and this effect is a limiting factor in the accuracy of Δt_{GO} determination.

One can then conclude that laminar/turbulent transition zone (2000 < Re < 4000) is probably the condition more closely related to MPFS.

Again, it should be stressed that a turbulent flow regime cannot be considered here, as the 0.221-s time interval corresponding to the GO period was no enough to permit a consistent regime to the established.

7. Fluidized beds

Fluidization is an operation which involves the flow of solids in contact with gas, liquid, or gas/liquid [44]. In flow analysis, it was recently exploited in a MPFS for zinc determination in plants involving in-line analyte separation by anion-exchange [45]. The fluidized bed was attained by introducing the pulsed flow at the bottom of a vertically positioned tubular resin mini-column. During the GO period, the solid particles were flushed upwards, and a steady circulating pattern was established; the suspended particles did not cause then any blockage or backpressure effects. During the STOP period, they tend to settle. In this way, a chaotic yet reproducible geometry was attained, and the main drawbacks inherent to ordinary in-line ion-exchange, such as high hydrodynamic pressure, preferential pathways, swelling effects and unavailability of some active sites were circumvented.

A remarkable feature of this strategy is that visual observation of the resin mini-column permitted one to put in evidence the turbulent mixing inherent to the pulsed flow.

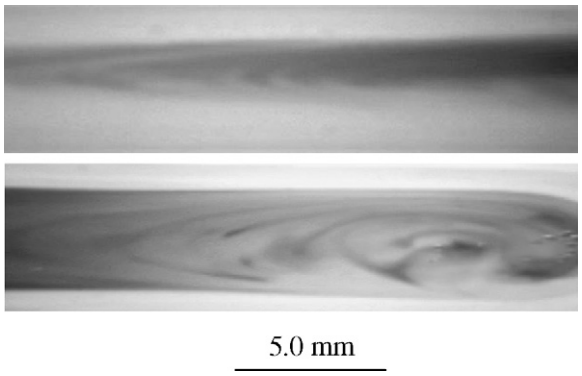

Fig. 8. Webcam images of the flowing sample under laminar (upper) and pulsed (lower) flow. Tube walls not shown; sample inlet at the right side; flow towards left. For details, see text.

8. Images of the flowing sample

As the dispersion phenomena involved in a laminar and in a pulsed flow are very distinct, a movie of the solutions mixing when exploiting different flow patterns can reveal important facts and confirm the results presented in the manuscript. To this end, the flow systems in Fig. 1 were used with the main reactor replaced by a glass cylinder (i.d.: 2.0 mm, length: 3.0 cm) positioned on a white background (paper sheet illuminated by an ordinary domestic fluorescent lamp). For image acquisition, a SPC 1300 NC Webcam, glass precision optics f:24 (Philips, China) was used.

Images of the flowing sample are shown in Fig. 8, revealing the laminar flow established inside the MCFS and the turbulent mixing (vortices) inside the MPFS. These vortices are perhaps the main contributors towards the improved radial mass transport. The entire video is available upon request.

9. Conclusions

Exploiting turbulent flows for minimizing sample broadening in a flow analyzer has been frequently born in mind. In this context, expressions such as *turbulent flow* and *turbulent mixing* have been often used in relation to pulsed flows [25]. In the present paper, the reader might imagine turbulent flows in MPFS.

However, a turbulent flow regime cannot be established, as the time span corresponding to the GO period is too short to characterize a flow regime, and other parameters such as *e.g.* viscosity and, more importantly, plasticity of the tubing walls play a significant role in the context. In addition, presence of vortices cannot be an indicative of turbulent flow regime, as vortices can be formed also in situations of low Reynolds numbers, meaning laminar flow regime.

One can then conclude that the enhanced radial mass transport inherent to a pulsed flow is due mainly to the turbulent mixing involved.

Acknowledgements

Partial support from FAPESP and from a bi-national consortium (CAPES/GRICES) is greatly appreciated.

References

[1] D. Betteridge, Anal. Chem. 50 (1978) 832A.
[2] F.A. Inon, M.B. Tudino, in: M. Trojanowicz (Ed.), Advances in Flow Analysis, Wiley VCH, Weinheim, 2008, p. 3 (Chapter 1).
[3] T. Korenaga, F.H. Shen, H. Yoshida, T. Takahashi, K.K. Stewart, Anal. Chim. Acta 214 (1988) 97.
[4] R.E. Thiers, R.R. Cole, W.J. Kirsch, Clin. Chem. 13 (1967) 451.
[5] S. Vicente, E.P. Borges, B.F. Reis, E.A.G. Zagatto, Anal. Chim. Acta 438 (2001) 3.
[6] L.R. Snyder, H.J. Adler, Anal. Chem. 48 (1976) 1017.
[7] J. Ruzicka, E.H. Hansen, Flow Injection Analysis, John Wiley & Sons, New York, 1981.
[8] D. Betteridge, B. Fields, Anal. Chem. 50 (1978) 654.
[9] E.N. Gaiao, R.S. Honorato, S.R.B. Santos, M.C.U. Araujo, Analyst 124 (1999) 1727.
[10] R. Tijssen, Anal. Chim. Acta 114 (1980) 71.
[11] H. Engelhardt, U.D. Neue, Chromatographia 15 (1982) 403.
[12] J.M. Reijn, H. Poppe, W.E. van der Linden, Anal. Chim. Acta 145 (1983) 59.
[13] J.M. Reijn, W.E. van der Linden, H. Poppe, Anal. Chim. Acta 123 (1981) 229.
[14] D. Slawinska, J. Slawinski, Anal. Chem. 47 (1975) 2101.
[15] T.J. Cardwell, R.W. Cattrall, G.J. Cross, J.R. O'Cornell, J.D. Petty, G.R. Scollary, Analyst 116 (1991) 1051.
[16] J.M.T. Carneiro, A.B.C. Dias, E.A.Z. Zagatto, J.L.M. Santos, J.L.F.C. Lima, Anal. Chim. Acta 531 (2005) 279.
[17] G.D. Clark, J.M. Hungerford, G.D. Christian, Anal. Chem. 61 (1989) 973.
[18] S.M.B. Brienza, R.P. Sartini, J.A. Gomes-Neto, E.A.G. Zagatto, Anal. Chim. Acta 308 (1995) 269.
[19] J. Ruzicka, L. Scampavia, Anal. Chem. 71 (1999) 257A.
[20] M. Hulsman, M. Bos, W.E. van der Linden, Anal. Chim. Acta 346 (1997) 351.
[21] S.R. Bysouth, J.F. Tyson, Anal. Chim. Acta 258 (1992) 55.
[22] S.M. Ramasamy, M.S.A. Jabbar, H.A. Mottola, Anal. Chem. 52 (1980) 2062.
[23] M.D.H. Silva, C. Pasquini, Anal. Chim. Acta 393 (1999) 121.
[24] T. Takayanagi, J. Flow Injection Anal. 25 (2008) 91.
[25] P.S. Francis, S.W. Lewis, K.F. Lim, K. Carlsson, B. Karlberg, Talanta 58 (2002) 1029.
[26] R.A.S. Lapa, J.L.F.C. Lima, B.F. Reis, J.L.M. Santos, E.A.G. Zagatto, Anal. Chim. Acta 466 (2002) 125.
[27] J.L.M. Santos, M.F.T. Ribeiro, J.L.F.C. Lima, A.C.B. Dias, E.A.G. Zagatto, Spectrosc. Lett. 40 (2007) 41.
[28] A.C.B. Dias, J.L.M. Santos, J.L.F.C. Lima, C.M. Quintella, A.M.V. Lima, E.A.G. Zagatto, Anal. Bioanal. Chem. 388 (2007) 1303.
[29] J.L.F.C. Lima, J.L.M. Santos, A.C.B. Dias, M.F.T. Ribeiro, E.A.G. Zagatto, Talanta 64 (2004) 1091.
[30] J. Ruzicka, Analyst 125 (2000) 1053.
[31] J. Ruzicka, E.H. Hansen, Anal. Chim. Acta 99 (1978) 37.
[32] K.L. Marques, C.K. Pires, J.L.M. Santos, E.A.G. Zagatto, J.L.F.C. Lima, Int. J. Environ. Anal. Chem. 87 (2007) 77.
[33] M.F.T. Ribeiro, A.C.B. Dias, J.L.M. Santos, E. Fernandes, J.L.F.C. Lima, E.A.G. Zagatto, J. Biomol. Screen 12 (2007) 875.
[34] E.R. Alves, P.R. Fortes, E.P. Borges, E.A.G. Zagatto, Anal. Chim. Acta 564 (2006) 231.
[35] E.R. Alves, M.A. Feres, E.A.G. Zagatto, J.L.F.C. Lima, Curr. Anal. Chem. 5 (2009) 65.
[36] M. Romerosaldana, A. Rios, M. Valcarcel, Fresenius J. Anal. Chem. 342 (1992) 547.
[37] J. Toei, Analyst 113 (1988) 475.
[38] J. Ruzicka, G.D. Marshall, Anal. Chim. Acta 237 (1990) 329.
[39] D. Betteridge, P.B. Oates, A.P. Wade, Anal. Chem. 59 (1987) 1236.
[40] J.A.V. Prior, J.L.M. Santos, J.L.F.C. Lima, J. Pharm. Biomed. Anal. 33 (2003) 903.
[41] E.A.G. Zagatto, H. Bergamin-Filho, S.M.B. Brienza, M.A.Z. Arruda, A.R.A. Nogueira, J.L.F.C. Lima, Anal. Chim. Acta 261 (1992) 59.
[42] W.J. Duncan, A.S. Thom, A.D. Young, Mechanics of Fluids, 2nd ed., Edward Arnold, London, 1970.
[43] J. Ruzicka, E.H. Hansen, Flow Injection Analysis, 2nd ed., Wiley-Interscience, New York, 1988.
[44] L.-S. Fan, Powder Technol. 88 (1996) 245.
[45] M.F.T. Ribeiro, A.C.B. Dias, J.L.M. Santos, J.L.F.C. Lima, E.A.G. Zagatto, Anal. Bioanal. Chem. 384 (2006) 1019.
[46] E.A.G. Zagatto, B.F. Reis, H. Bergamin-Filho, Anal. Chim. Acta 226 (1989) 129.